



## REGULAR ARTICLE

# Influence of Microsecond Pulse Helium Plasma Flow on the Surface Morphology and Crystal Structure of the Photovoltaic Converters Based on CdS/CdTe

G.S. Khrypunov<sup>1,2\*</sup> , M.M. Harchenko<sup>1</sup>, A.V. Meriuts<sup>1</sup>, J.F. Carlin<sup>2</sup>, V.A. Makhlai<sup>3</sup>, S.S. Herashchenko<sup>3</sup>, S.L. Abashin<sup>4</sup>, S.V. Surovitskiy<sup>1</sup>, A.O. Pudov<sup>3</sup>, A.I. Dobrozhan<sup>1</sup> 

<sup>1</sup> National Technical University «Kharkiv Polytechnic Institute», 61002 Kharkiv, Ukraine

<sup>2</sup> Ecole Polytechnique Fédérale de Lausanne, CH-1015 Lausanne, Switzerland

<sup>3</sup> National Science Center “Kharkiv Institute of Physics & Technology”, 61108, Kharkiv, Ukraine

<sup>4</sup> National Aerospace University “Kharkiv Aviation Institute”, 61070, Kharkiv, Ukraine

(Received 10 January 2024; revised manuscript received 14 June 2024; published online 28 June 2024)

The influence of pulsed helium plasma irradiation, with a 10  $\mu\text{s}$  duration and a surface energy load of 0.2 MJ m<sup>-2</sup>, on the elemental and phase composition, surface morphology and crystal structure of thin-film heterosystems based on CdS/CdTe was studied. The cadmium sulphide and cadmium telluride layers were deposited by condensation via a hot wall method onto a glass substrate covered with an FTO layer. It was found that after one pulse, the device structure remains in working condition. An increase in the irradiation dose leads to surface sputtering, the formation of through pores 0.5 – 2  $\mu\text{m}$  in size, and a microcracks network with two characteristic scales. One crack network is formed in the glass substrate, and the second network is formed with cracks in the CdTe film. It is shown that the thermal effect of plasma stimulates the diffusion of sulphur; as a result, the proportion of CdTe<sub>1-x</sub>S<sub>x</sub> solid solutions formed in the process of obtaining the CdS/CdTe heterosystem increases. In addition, the sulphur content increases in these solid solutions, which leads to their decomposition with the separation of the CdS<sub>1-y</sub>Te<sub>y</sub> solid solution phase. These solid solutions migrate to the CdTe surface through cracks and are observed as separate crystals.

**Keywords:** Photovoltaic converters, Thin-film, Cadmium telluride, Radiation resistance, Solid solutions.

DOI: [10.21272/jnep.16\(3\).03001](https://doi.org/10.21272/jnep.16(3).03001)

PACS numbers: 81.05.Dz, 81.40.Wx

## 1. INTRODUCTION

Currently, cadmium telluride as a base material is becoming an alternative to silicon for a number of device structures for use under conditions of increased radiation exposure [1]. Single-crystal detectors of  $\gamma$ ,  $\alpha$ , proton radiation based on CdTe and CdZnTe semiconductors have long been used in medicine and astrophysics, for the radiometric control at nuclear power plants, at the nuclear fuel production and processing enterprises, in the environmental monitoring, as well as in the spectrometric systems for single-photon emission tomography of radioactive waste and in the nuclear-physical methods of elemental analysis [2,3]. Such widespread use is due to the high radiation absorption efficiency of these materials, and good energy resolution of the respective devices. When using cadmium telluride as the base layers of radiation detectors, due to the higher atomic numbers of tellurium and cadmium, this semiconductor has a greater radiation stopping efficiency, which allows to create detectors for a wide range of energies from 5 keV to 2 MeV. The band gap of cadmium telluride material ( $E_g = 1.5$  eV at 300 K) is significantly higher than that of silicon ( $E_g \sim 1.1$  eV at 300 K). As a result, X-ray detectors based on cadmium telluride can much more

effectively operate at room temperature [3] due to lower leakage current values. All this makes it possible to create large-area cadmium telluride based detector arrays [4,5]. Recently, there has been interest in using thin layers of this base material in the detectors, which increases the spatial resolution and, accordingly, the image quality. In Ref. [6], radiation-resistant polycrystalline thick CdTe films with a thickness of 300  $\mu\text{m}$  were used as the detectors on the Large Hadron Collider. In the framework of space missions to study the Sun [7,8], the use of radiation-resistant solar cells (SCs) also remains essential. Lately, some articles have been published describing the usage of thin-film SCs based on cadmium sulphide and cadmium telluride for radiation detectors creation [9]. In the detectors of this type, the radiation level is estimated from the value of photocurrent generated under the exposure to radiation. The high radiation resistance of the CdTe material itself has been known for a long time [10], but, for specific applications and concrete devices, the radiation resistance is important [11] and needs to be investigated. Previous studies of radiation resistance of CdS/CdTe heterojunction structures allow to conclude that they have sufficient radiation resistance for space use. For example, in Ref. [12], CdTe solar cells of 10 to 12%

\* Correspondence e-mail: [khrip@ukr.net](mailto:khrip@ukr.net)



efficiency were irradiated with protons of high energy (5 to 15 MeV) and fluence ( $10^{11} \text{ cm}^{-2}$  to  $10^{13} \text{ cm}^{-2}$ ) to determine their radiation resistance.

In the majority of the published radiation resistance studies, particles with high energies and relatively not very high flux densities and irradiation doses were usually used. The low densities typically allow to record changes in the electrical characteristics of the device structures, but they are not always sufficient to establish degradation mechanisms. At the same time, it follows from such studies, that the primary influence on degradation is not so much the energy of the particles in the flow as the accumulated radiation dose. In Ref. [13], we began our investigation of influence of high-intensity plasma flows on CdS/CdTe, with the focus on the irradiation with hydrogen plasma and its effects on the photoelectric properties and crystal structure of these device structures. In that study, the irradiation doses were established, at which structural changes at the CdS/CdTe interface begin to occur, which causes a decrease in the output photoelectric parameters of such device structures. Also, the mechanisms that lead to the structural changes at the CdS/CdTe interface and to the deterioration of the photoelectric parameters of such device structures were established.

In this article, we present a further study of the influence of critical doses of, in this case, helium plasma irradiation on the radiation resistance of the CdS/CdTe-based device structures, which is also relevant both from the point of view of the development of radiation semiconductor materials science and from the point of view of the development of both thin-film solar cells and radiation detectors. The study of the mechanisms that lead to the degradation of the electrical characteristics will make it possible to manufacture more radiation-resistant device structures in the future.

## 2. EXPERIMENTAL

Cadmium telluride thin-film photovoltaic converters (PVCs) were formed on a glass substrate with a previously applied transparent and conductive Fluorine-doped Tin Oxide (FTO) layer, which performs the functions of a front electrode in the device structure. The surface resistance of the FTO layer was  $10 - 12 \Omega/\square$ , and the average transmission coefficient in the visible part of the spectrum was 80 – 85%. The sequence of operations in the manufacture of the solar cells is as follows: deposition of CdS and CdTe layers; the “chloride” treatment; creating a back contact.

The cadmium sulfide and cadmium telluride layers were deposited by condensation in a hot wall method, which allows deposition under the conditions close to the thermodynamical equilibrium. The layers were deposited sequentially without depressurization of the working volume at a residual gas pressure of no higher than  $10^{-5} \text{ mm Hg}$ . Two separate graphite chambers located in the working volume of an industrial vacuum installation were used. The methodology for depositing the layers is described in detail in Ref. [14].

During the CdS layer deposition, the temperatures of the evaporator zone and the substrate were  $590 \text{ }^\circ\text{C}$  and  $395 \text{ }^\circ\text{C}$ , respectively, which corresponds to quasi-equilibrium condensation conditions. With a

condensation process duration of 15 min,  $0.3 - 0.32 \mu\text{m}$  thick CdS films were obtained.

The CdTe layers were deposited at a temperature of the evaporation zone of  $520 \text{ }^\circ\text{C}$  and a substrate temperature of  $497 \text{ }^\circ\text{C}$ . In this temperature regime, with a duration of the condensation process of 7 min, CdTe films with a thickness of  $3.8 - 4 \mu\text{m}$  and grain sizes at the surface of  $3 - 5 \mu\text{m}$  were obtained.

The “chloride” treatment consisted in the deposition of a  $\text{CdCl}_2$  film on the surface of a CdTe film by thermal vacuum evaporation without heating the substrate and annealing the entire structure in air at a temperature of  $410 - 415 \text{ }^\circ\text{C}$  during 20 min. After the annealing, the surface was etched in a solution of bromine in methanol to remove the products of the chemical reactions.

The back contact was formed by depositing copper and gold films with a thickness of 11 nm and 50 nm, respectively, followed by the annealing of the structure in air at a temperature of  $230 \text{ }^\circ\text{C}$  for 20 minutes. The copper and gold films were deposited by vacuum thermal evaporation in a single cycle at a pressure of no higher than  $10^{-5} \text{ mm Hg}$  without heating the substrate. The thickness of the layers was monitored by a quartz thickness gauge. The finished device structure has the following sequence of thin-film layers: glass

substrate/FTO( $0.5 \mu\text{m}$ )/CdS( $0.3 - 0.32 \mu\text{m}$ )/CdTe( $3.8 - 4 \mu\text{m}$ )/ Cu( $\sim 11 \text{ nm}$ )/Au( $\sim 50 \text{ nm}$ ),

which totals  $\sim 5 \mu\text{m}$  without the substrate.

The photovoltaic converters based on the CdS/CdTe heterosystem were exposed to compressed plasma fluxes in the magnetoplasma compressor (MPC) to study the effect of the helium plasma irradiation. The irradiation was performed in the pulsed mode, and the discharge half-period was about  $10 \mu\text{s}$ . The experiments were carried out using pure helium at an initial pressure of  $266.64 \text{ Pa}$ . The average plasma temperature ranged from  $60 - 120 \text{ eV}$ . The particle flux during the pulse was  $\approx 10^{21} \text{ m}^{-2}\text{s}^{-1}$ , and the energy density absorbed by the surface was  $0.2 \text{ MJ m}^{-2}$ . The samples were irradiated with 5 helium plasma pulses. Before each pulse, the temperature of the sample surface was at room temperature and increased during plasma exposition. The time intervals between pulses were sufficient to cool the samples to room temperature.

The phase composition and crystalline structure of the obtained device structures were studied by X-ray diffraction. Diffraction patterns were registered with a DRON and D8 DISCOVER (BRUKER) type diffractometers according to the  $\theta - 2\theta$  scanning scheme in the radiation of a Cu anode using digital registration. The diffraction patterns were processed using the New\_Profile 3.5 software package.

The predominant orientation of the films was studied by the analytical processing of the registered diffraction maxima by using Bragg – Brentano focusing. Texture coefficients ( $C_i$ ) were calculated and the direction and degree of predominant orientation of films ( $G$ ) were determined as in Ref. [15].

The precision determination of the lattice period of the base layers of cadmium telluride was carried out by using the Nelson – Riley extrapolation function  $f(\theta) = (\cos^2\theta \sin\theta + \cos^2\theta' \theta)/2$ .

The surface morphology was studied by scanning electron microscopy (SEM). Elemental analysis of the surface was carried out by Auger electron spectroscopy.

### 3. RESULTS AND DISCUSSION

In the initial state, the device structures had photosensitivity and could be used as SCs and radiation sensors of  $\alpha$ -particles [13]. The free surface of the cadmium telluride films was smooth, had a typical grey colour, and the average grain size of the layers was  $1 - 3 \mu\text{m}$ . The surface of the rear Au/Cu contact was mirror-like with a characteristic yellow colour. As evidenced by the results of microanalysis, the elemental composition of both areas corresponded to the stoichiometric phase of CdTe, and the back contact area contained copper and gold, respectively.

During the irradiation of the samples, it was established that a ten-microsecond helium plasma pulse with a surface energy load of  $0.2 \text{ MJ m}^{-2}$  leads to an insignificant, although noticeable decreasing of the solar cell efficiency by 0.5 %. The irradiation with the total of three pulses resulted in a significant deterioration of the photoelectric parameters of the PVCs, which makes such structures no longer practical to use as solar cells or radiation detectors. At the same time, no noticeable changes in surface morphology and structure (within the measurement accuracy) were detected after the first pulse. After the total of three pulses, darkening of the contact area was observed, and changes in the phase

composition at the CdS/CdTe heterojunction were detected. To intensify the processes and more precisely establish the mechanisms of degradation, the irradiation dose was increased to the total of five pulses. After such a critical dose, the surface morphology, elemental and phase composition, as well as the crystal structure of the CdS/CdTe film heterosystem were studied.

Fig. 1 shows a photo of the PVC samples' surface after the irradiation with the total of 5 helium plasma pulses with the parameters described above. As can be seen, the irradiation leads to the formation of defects in the base and contact layers: through pores (Fig. 1a, b), a grid of cracks with two characteristic scales (Fig. 1a, c), the change in the morphology of the back contact area (Fig. 1a, it becomes gray and bumpy instead of a smooth mirror-yellow surface).

The pores have a form of punctures with clear edges, the size of each is  $0.5 - 2 \mu\text{m}$ . The highest pore density is observed in the areas, where the back contact has been formed, and, in some places, the density reaches  $8500 \text{ mm}^{-2}$ . Fig. 1d shows an image of the free substrate surface, on which the CdS/CdTe heterostructure was not obtained (an edge area of the substrate), after the high-energy plasma irradiation. A comparison of the scales of the crack networks on the surface of the substrate and that in the CdTe film shows that the cracks of the thin film with the large scale are inherited from the substrate material. The cracking on the smaller scale (which is absent on the substrate) is associated with cracking of the base CdTe layer film itself.

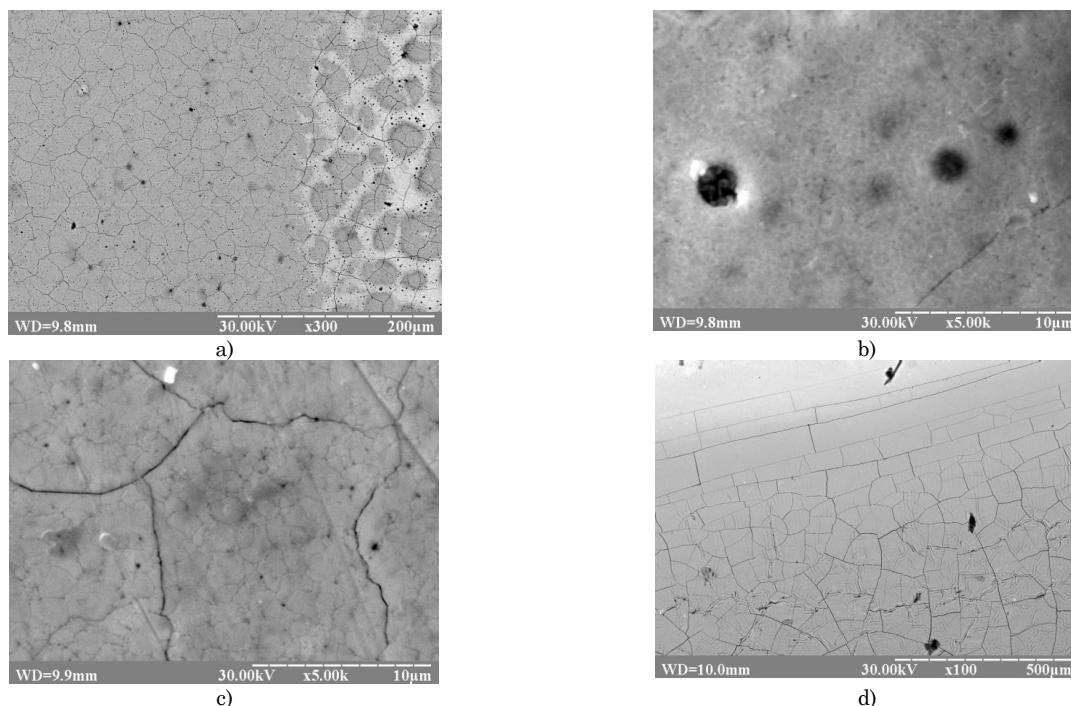


**Fig. 1** – The surface morphology after the irradiation with 5 helium plasma pulses with a surface energy load of  $0.2 \text{ MJ m}^{-2}$  each: a) border between the surface areas of the CdTe base layer and Cu-Au back contact; b) the through pores; c) a cracks' network on the surface of the CdTe base layer; d) the free surface of the substrate after the irradiation.

Our studies have shown that, after the irradiation, there was no clearly defined relief on the most part of the contact-free surface of the CdTe base layer, similarly to the initial state, and the average grain size remained the same

( $3 - 5 \mu\text{m}$ ). However, the appearance of new formations in some areas of the surface, approximately round in shape and up to  $200 \mu\text{m}$  in diameter, was observed. Such formations also appear in those areas where the back

contact was formed (see Fig. 2a, around point 3).

The change in the morphology of the back contact after the irradiation consists in the fact that there appeared breaks of the contact layer continuity and the formation of a relief in it (Fig. 2a), compared to the initial state, in which the metal area was mirror smooth. The shape of the relief corresponds to the liquid phase formation, followed by its crystallization without completely wetting of the base CdTe surface. These relief elements in the backscattered electrons image (Fig. 2b) have a lighter shade compared to the base layer surface, which indicates the presence of heavy chemical elements. Table 1 shows the results of the microanalysis of the chemical composition of the surface in the contact region. Three characteristic points were selected in this section. The first one (Point 1 in Fig. 2a) is located on the surface of the CdTe base layer, which seems to have become free from the contact material after the irradiation. It is seen from Table 1 that such areas indeed contain only Cd and Te, that is, they correspond to the CdTe phase without other elements. In the second type of area (Point 2 in Fig. 2a), the signals from Au are observed, as well as from Cd and Te. The CdTe-Au state diagram is of the eutectic type (a eutectic temperature is 1083 K). At temperatures 873 – 1273 K, the solubility of gold in cadmium telluride increases by more than an order of magnitude and is

described by the formula  $c_{Au} = 6.2 \cdot 10^{20} \exp(-E/k_B T)$ , where  $E = 0.59$  eV is the activation energy [16]. Based on this, we can assume that, after the helium plasma irradiation, there is a eutectic melting at the CdTe/Au heterointerface in the back contact area, and, as a result, the gold contact with a thickness of 50 nm is gathered in drops on the cadmium telluride surface (of course, it is also partially sputtered off by the plasma flow) and forms the areas of CdTe enriched with Au (Point 2 in Fig. 2a) and the pure CdTe open surface areas (Point 1 in Fig. 2a).

On the SEM image of the surface of the device structure (Fig. 2), one can also see the elements formed as a result of the plasma irradiation. It is seen that these elements were formed only above the cracks of the base layer and consist of crystals 2-4  $\mu\text{m}$  in size. Some of these crystals have a clear faceted rectangular shape. The formation of such crystals is observed both on the free surface and the back contact areas. More often, these formations are gathered in disk-shaped accumulations with a diameter up to 200 microns as shown in Fig. 2a. But there are also individual crystals. In the backscattered electrons image, these elements have a darker contrast, which indicates the content of a light chemical element. The estimation of the total area of these formations shows that they occupy less than 1% of the total surface.

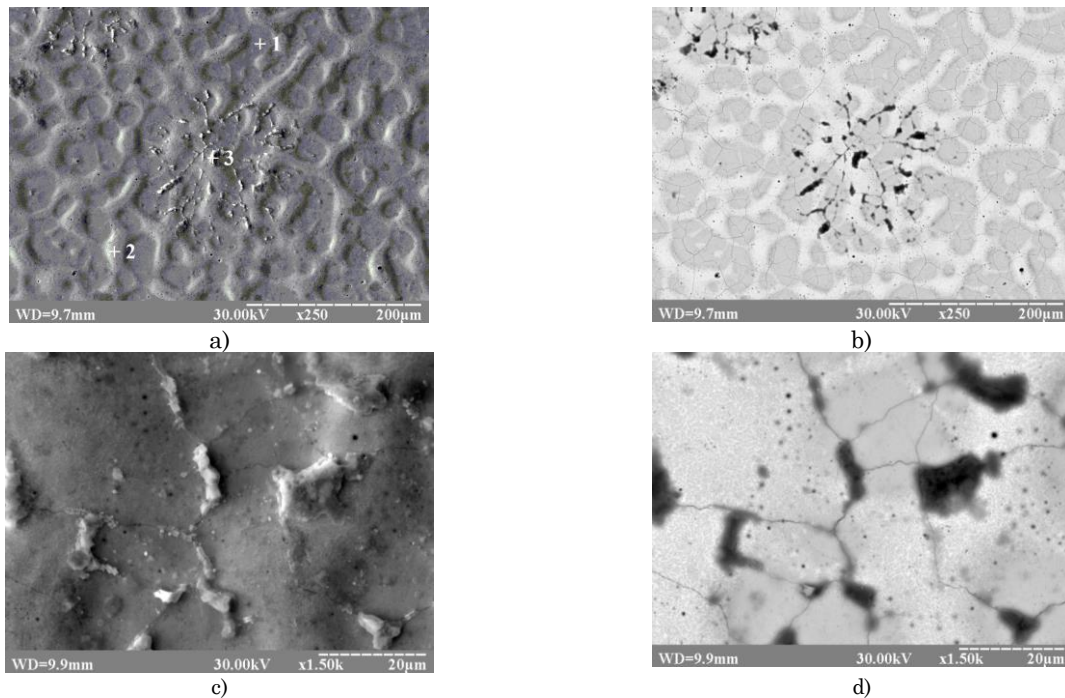


**Fig. 2** – An image of the back contact surface after the irradiation with the total of 5 pulses of high-energy helium plasma: a) the secondary electrons image; b) the backscattered electrons image; c) the area of formation of the  $\text{CdS}_{1-y}\text{Te}_y$  additional phase on the PVC surface in the secondary electrons mode; d) same as c) only in the backscattered electrons mode.

In comparison with the results from the PVC free surface, for these elements (Table 1, Point 3) there is a decrease in the concentration of Te relative to Cd and the presence of S with a concentration, that exceeds the concentration of Te. The results of the elemental composition

determination indicate the formation of  $\text{CdS}_{1-y}\text{Te}_y$  solid solutions, in which S atoms in the CdS lattice are replaced by Te atoms. In the back contact area, this phase contains copper, which is not present in such formations on the CdTe base layer surface.

**Table 1** – Elemental analysis of the PVC surface after the irradiation with the total of 5 pulses of high-energy helium plasma (Fig. 2a)

| Element | Point 1 |       |        | Point 2 |       |        | Point 3 |       |        |
|---------|---------|-------|--------|---------|-------|--------|---------|-------|--------|
|         | I, imp. | C, %  | At. %  | I, imp. | C, %  | At. %  | I, imp. | C, %  | At. %  |
| Cd      | 15291   | 54.41 | 57.537 | 11061   | 42.56 | 47.653 | 16743   | 74.32 | 58.636 |
| Te      | 12383   | 45.59 | 42.463 | 12819   | 45.07 | 44.445 | 2583    | 12.89 | 8.960  |
| S       | -       | -     | -      | -       | -     | -      | 10287   | 10.62 | 29.385 |
| Au      | -       | -     | -      | 939     | 12.37 | 7.901  | -       | -     | -      |
| Cu      | -       | -     | -      | -       | -     | -      | 550     | 2.16  | 3.019  |

Solid solutions with limited mutual solubility can be formed in the CdTe-CdS system [16-18]. According to the phase diagram of the CdTe-CdS system [18], which was constructed at temperatures above 700 °C, the maximum solubility of sulphur in cadmium telluride layers is 20 %. In this case, CdTe<sub>1-x</sub>S<sub>x</sub> (x < 0.2) solid solutions have the sphalerite structure. The maximum solubility of tellurium in cadmium sulphide is 10%. Solid solutions CdS<sub>1-y</sub>Te<sub>y</sub> (y < 0.1) have a wurtzite structure. A feature of the phase diagram of this system at lower temperatures is a decrease in the maximum solubility of sulphur in CdTe [19, 20]. It was shown [21] that as the temperature of CdTe formation decreases to 370°C, the solubility of sulphur in cadmium telluride decreases to 3%. In Ref. [22], in which SCs based on CdTe/CdS were obtained at deposition temperatures of 600°C, CdTe<sub>1-x</sub>S<sub>x</sub> layers with x = 0.07 were formed at the interface. The authors of this work believe that this value (7%) is the limiting solubility of sulphur in film layers of cadmium telluride under such conditions. It was shown in Ref. [23] that, as a result of interfacial interaction during the formation of thin-film SCs based on CdTe/CdS, interlayers of their solid solutions are formed after the “chloride” treatment. In this case, the limiting solubility of the components depends on the temperature [16,19].

The study of the crystal structure of film layers of supersaturated solid solutions CdTe<sub>1-x</sub>S<sub>x</sub> (0.1 < x < 0.9) obtained at deposition temperatures below 200 °C showed that heating to temperatures above 300 °C leads to the decomposition of solid solutions. As a result of decomposition, a heterogeneous thin film structure is formed from two solid solutions: one based on cadmium telluride and the other based on cadmium sulphide [24]. Studies of the lattice period of the solid solutions indicate that the change in the lattice period (a) with a change in the composition of the CdTe<sub>1-x</sub>S<sub>x</sub> solid solution of the cubic modification and the lattice periods (a, c) of the CdS<sub>1-y</sub>Te<sub>y</sub> solid solution of the hexagonal modification in the region of limited solubility, corresponding to the Vegard rule [25]. Studies of diffusion processes indicate that in the thin-film composition, during the formation of CdTe-CdS SCs, diffusion of sulphur into the CdTe layer is observed; no diffusion of tellurium into the CdS layer was recorded [26]. The authors of Ref. [27] reported that the “chloride” heat treatment of the CdTe-CdS system in air, which is obligatory in the manufacture of highly efficient SCs, causes the presence of oxygen atoms at the sites of the tellurium sublattice on the grain-boundary surface of the base layer. This leads to the fact that the rate of diffusion of sulphur atoms in CdTe via grain boundaries is lower than the diffusion rate in the grain bulk. Therefore, the dominant mechanism of sulphur diffusion is diffusion in the volume of grains. Such a mechanism

of sulphur diffusion was experimentally confirmed in Ref. [28]. The authors of this publication recorded the presence of sulphur after heat treatment of the CdTe-CdS system only in the bulk of cadmium telluride grains.

A comparison of the obtained experimental results with the literature data presented above indicates that after the irradiation with helium plasma, the formation of CdTe<sub>1-x</sub>S<sub>x</sub> solid solutions occurs at the CdS/CdTe heterointerface. In this case, as a result of a higher heating temperature of the sample during the irradiation with helium plasma compared to the temperature of the “chloride” treatment, it can be assumed that solid solutions are formed with a higher sulphur content than in the initial state, and CdS<sub>1-y</sub>Te<sub>y</sub> solid solutions based on CdS are formed locally. CdTe<sub>1-x</sub>S<sub>x</sub> and CdS<sub>1-y</sub>Te<sub>y</sub> solid solutions have melting points lower than that of the cadmium telluride upper layer, so, in the process of formation, they turn into a liquid state, absorbing part of the plasma energy for their melting. As a result, a liquid phase of solid solutions of CdS<sub>1-y</sub>Te<sub>y</sub> forms under the cadmium telluride layer, which has a lower density (CdS density is 4.82 g/cm<sup>3</sup>) than CdTe and CdTe<sub>1-x</sub>S<sub>x</sub> (CdTe density is 5.86 g/cm<sup>3</sup>). Under by the plasma flow pressure and due to the capillary effect, these solid solutions go up through cracks and crystallize (Point 3 in Fig. 2a). As the elemental analysis shows, point 3 (CdS<sub>1-y</sub>Te<sub>y</sub> solid solutions) has a different tellurium content, which can be explained by the strongly nonequilibrium conditions of the solution formation.

The elemental composition investigation results were supplemented by the X-ray diffraction analysis. Fig. 3 shows the XRD patterns of PVC based on CdTe obtained by the hot wall method in the initial state and after helium plasma radiation with the total of 5 pulses.

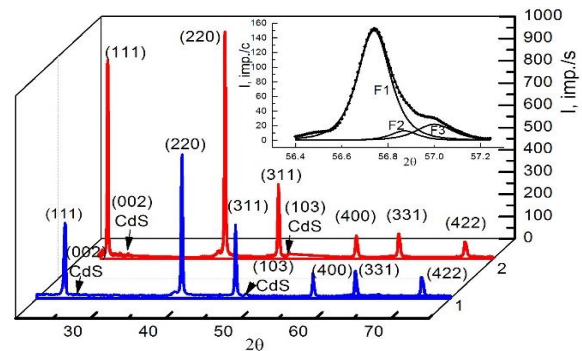


**Fig. 3** – The XRD patterns of the PVC sample: 1 – in the initial state, 2 – after the high-energy helium plasma irradiation with the total of 5 pulses (in Cu K<sub>α</sub> radiation). The inset: the reflex from the (400) plane in the initial sample state

When analysing the shape of the diffraction peaks, the positions of which correspond to CdTe, it was found that they contained three components. In the following

discussion, we will denote these components as phases F1, F2, and F3. As was shown in [15], when studying CdS/CdTe film solar cells, the separation of the peaks is due to the formation of  $\text{CdTe}_{1-x}\text{S}_x$  solid solutions, which have smaller interplanar spacings. The lattice periods of the detected phases were determined. Before the irradiation, the lattice periods of the F1, F2, and F3 phases were 6.4830 Å, 6.4720 Å, and 6.4579 Å, respectively (Fig. 4a). According to reference data (PCPDFWIN #15-0770 card), the CdTe lattice period is 6.481 Å, so the F1 phase was identified as pure CdTe. Two other phases, according to Vegard's rule ( $a_{\text{CdS}_x\text{Te}_{1-x}} = xa_{\text{CdS}} + (1-x)a_{\text{CdTe}}$ ), were identified as  $\text{CdTe}_{1-x}\text{S}_x$  solid solutions with a sulphur concentration of ~3 % for F2 and ~8 % for F3.

An analysis of the integral intensity of the diffraction peaks showed that, after the irradiation, the ratio between the phases F1, F2, and F3 changes towards an increase of the portion of the solid solutions. Thus, after

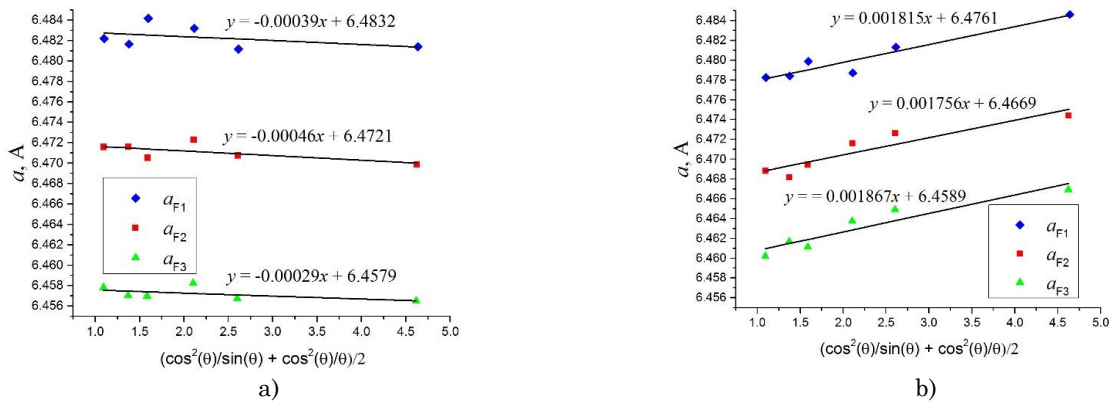


**Fig. 4** – Precise determination of the lattice constant in the initial state (a) (F1 – CdTe, F2 and F3 – solid solutions of  $\text{CdTe}_{1-x}\text{S}_x$ ), and after the irradiation (b) (F1, F2, F3 – solid solutions of  $\text{CdTe}_{1-x}\text{S}_x$ ) with the total irradiation dose (particle fluence) of  $5 \cdot 10^{16} \text{ m}^{-2}$

The increase in the intensity of diffraction reflections from the cadmium sulphide layer after the irradiation can be explained both by a decrease in the thickness of the CdTe layer covering it due to partial sputtering off, and by the emergence of the  $\text{CdS}_{1-y}\text{Te}_y$  solid solutions on the surface with a lattice period close to that of CdS. The shift of diffraction maxima towards larger angles indicates an increase in interplanar distances, which may be due to the replacement of sulphur atoms by tellurium atoms, which have a larger atomic radius, during the formation of the  $\text{CdS}_{1-y}\text{Te}_y$  solid solutions. The low intensity of the diffraction peaks of cadmium sulphide does not allow their reliable processing for the study of the solid solutions based on them.

After the irradiation, the integral full width at half maximum (FWHM) of all peaks increased for all detected phases, except for the (111) diffraction peak, for which the integral FWHM decreased for the F2 and F3 phases. An analysis of the XRD pole density for the sample shows that, after the irradiation with helium plasma, the preferred orientation for the F2 and F3 phases in the [220] direction doubled and significantly decreased in the [422] direction (more than two times for F2, and 1.5 times for F3). There were no changes in the preferred orientation for the main CdTe phase. Since the [422] direction is characterized by the minimum probability of the formation of twins and stacking faults, the decrease in the intensity of the peak indicates an

increase in the concentration of structural defects of this type after the irradiation with helium ions.

the irradiation, the relative content of the F1 phase in the test sample decreases from 84% to 72%. For the phases F2 and F3, there is an increase from 7% to 17% and from 9% to 12%, respectively. At the same time, the composition of the phases also changes. After the helium plasma irradiation, the lattice period of the CdTe base layer decreased from 6.4830 Å to 6.4761 Å. Such a change in the lattice period of the main phase, according to the Vegard law, may indicate that almost the entire CdTe base layer has turned into  $\text{CdTe}_{1-x}\text{S}_x$  solid solutions with a sulphur concentration of about 1.5% ( $x = 0.0148$ ) as a result of bulk diffusion of sulphur into the cadmium telluride layer. For  $\text{CdTe}_{1-x}\text{S}_x$  solid solutions of the F2 phase, which were at the CdS/CdTe interface in the initial state, the lattice period decreased from 6.4720 Å to 6.4669 Å, which corresponds to an increase in the sulphur quantity from 3% ( $x = 0.0297$ ) to 3.7% ( $x = 0.0372$ ).

increase in the concentration of structural defects of this type after the irradiation with helium ions.

#### 4. CONCLUSIONS

The studies showed that device structures based on CdS/CdTe have high radiation resistance. The irradiated samples withstood 5 MPC helium plasma impacts with a 10  $\mu\text{s}$  duration and a surface energy load of 0.2  $\text{MJ m}^{-2}$ . The accumulated irradiation dose (particle fluence) amounted to  $5 \cdot 10^{16} \text{ m}^{-2}$ . When the critical radiation dose is exceeded, the crystal structure and surface morphology change, which is accompanied by a catastrophic deterioration of all the electrical characteristics of the device structure.

Irradiation with a helium plasma flow leads to the sputtering off of the surface, and, in the contact area at high doses, cracking of the film, formation of through pores and eutectic melting at the CdTe/Au interface occur, as a result of which the gold film collects in droplets. Thermal influence leads to the intensification of sulphur diffusion into the cadmium telluride layer, which has two consequences. First, almost the entire base layer of CdTe is transformed into the solid solutions of  $\text{CdTe}_{1-x}\text{S}_x$  with a minimum sulphur concentration of ~1.5%. Secondly, in the CdTe-based solid solutions, i.e.  $\text{CdTe}_{1-x}\text{S}_x$ , which are formed at the CdS/CdTe boundary during the manufacture of the device structure, the

sulphur content increases. When the sulphur concentration in the solid solutions of  $\text{CdTe}_{1-x}\text{S}_x$  exceeds the equilibrium solubility limit, their disintegration occurs with the release of a phase of solid solutions based on CdS, i.e.  $\text{CdS}_{1-y}\text{Te}_y$ . The phase of  $\text{CdS}_{1-y}\text{Te}_y$  solid solutions is observed on the cadmium telluride film surface. We claim that this phase, under the plasma flow

action due to the capillary effect, comes to the surface through the cracks in the CdTe film due to the fact that it has a lower melting temperature than all other phases.

The obtained results show that one of the factors of degradation of PVCs based on CdS/CdTe can be the disintegration of solid solutions, that are formed at the heterosystem boundaries during their manufacture.

## REFERENCES

1. T. Takahashi, S. Watanabe, *IEEE T Nucl Sci* **48** No 4, 950 (2001).
2. S. Del Sordo, L. Abbene, E. Caroli, A.M. Mancini, A. Zappettini, P. Ubertini, *Sensors* **9** No 5, 3491 (2009).
3. V.Ye. Kutny, A.V. Rybka, L.N. Davydov, A.A. Zakharchenko, D.V. Kutnay, A.S. Abyzov, *Ionoziring radiation detectors based on cadmium-zinc telluride*. (Kharkiv: Madrid Printing House: 2021).
4. L. Brombal, S. Donato, F. Brun, P. Delogu, V. Fanti, P. Oliva, L. Rigon, V. Di Trapani, R. Longo, B. Golosio, *J. Synchrotron Rad* **25** No 4, 1068 (2018).
5. M. Sammartini, M. Gandola, F. Mele, B. Garavelli, D. Macera, P. Pozzi, G. Bertuccio, *Nucl Instrum Meth A*, **910**, 168 (2018).
6. A. Brambilla, S. Renet, M. Jolliot, E. Bravin, *Nucl Instrum Meth A* **591** No 1, 109 (2008).
7. R. Bandyopadhyay, W.H. Matthaeus, D.J. McComas, R. Chhiber, A.V. Usmanov, J. Huang, R. Livi, D.E. Larson, J.C. Kasper, A.W. Case, M. Stevens, P. Whittlesey, O.M. Romeo, S.D. Bale, J.W. Bonnell, T. Dudok de Wit, K. Goetz, P.R. Harvey, R.J. MacDowall, D.M. Malaspina, M. Pulupa, *ApJL* **926** No 1, 1 (2022).
8. C. Li, C. Fang, Z. Li, M.-D. Ding, P.-F. Chen, Z. Chen, L.-K. Lin, C.-Z. Chen, C.-Y. Chen, H.-J. Tao, W. You, Q. Hao, Y. Dai, X. Cheng, Y. Guo, J. Hong, M.-J. An, W.-Q. Cheng, J.-X. Chen, W. Wang, W. Zhang, *Res. Astron. Astrophys.* **19** No 11, 165 (2009).
9. N.R. Paudel, D. Shvydka, E.I. Parsai, *J Appl Clin Med Phys.* **17** No 5, 500 (2016).
10. K. Zanio, F.H. Pollak, *Physics Today* **31** No 8, 53 (1978).
11. A. Owens, *Semiconductors Radiation Detectors*. (Boca Raton: CRC Press: 2019).
12. A. Romeo, D.L. Batzner, H. Zogg, A.N. Tiwari, *Proceeding of 17th European Photovoltaic Solar Energy Conversion and Exhibition*, 540 (Munich: WIP-Renewable Energies: 2001).
13. A.V. Meriuts, M.M. Kharchenko, G.S. Khrypunov, A.O. Pudov, V.A. Makhlai, S.S. Herashchenko, S.A. Sokolov, A.V. Rybka, V.E. Kutny, I.V. Kolodiy, A.I. Dobrozhan, A.V. Kosinov, M.G. Khrypunov, *J Appl Phys.* **132** No 10, 104501 (2022).
14. M.M. Kharchenko, *Phys. Chem. Solid St.* **8** No 4, 718 (2007).
15. H.R. Moutinho, F.S. Hasoon, F. Abulfotuh, K. Kazmerski, *J Vac Sci Technol A* **13** No 6, 2877 (1995).
16. V.N. Tomashik, V.I. Gryshev, *State diagram of the systems based on the A2B6 semiconductor compounds*. (Kiev: Naukova Dumka: 1982).
17. D.W. Lane, G.J. Conibeer, D.A. Wood, K.D. Rogers, P. Capper, S. Romani, *J Cryst Growth* **197**, 743 (1999).
18. S.Y. Nunoue, T. Hemmi, E. Kata, *J Electrochem Soc*, **137** No 4, 1248 (1990).
19. K. Ohata, J. Saraie, T. Tanaka, *JJAP* **12** No 8, 1198 (1973).
20. D.W. Lane, K.D. Rogers, J.D. Painter, D.A. Wood *Thin Solid Films* **361-362**, 1 (2000).
21. B.E. McCandless, G.M. Hanket, D.G. Jensen, R.W. Birkmire, *J Vac Sci Technol A* **20** No 4, 1462 (2002).
22. D. Bonnet, *14 European Photovoltaic Solar Energy Conference: Proceeding of the conference*, 2688 (Munich: WIP-Renewable Energies: 1997).
23. B.E. McCandless, R.W. Birkmire, *26-th IEEE Photovoltaic Special Conference: Proceeding of the International Conference*, 307 (Anaheim: IEEE:1997).
24. V.Ya. Vitiuk, V.A. Sanitarov, N.N. Zavlenko, I.P. Kalinkin *Newsletter of the Academy of Science of USSR. Nonorganic materials*, **18** No 9, 1514 (1982).
25. O.M. Melender-Lira, I. Hernander-Calderon, *First World Conference on Photovoltaic Energy Conversion (WCPEC)* 369 (Hawaii: IEEE:1994).
26. B.E. McCandless, M.G. Engelmann, R.W. Birkmire *J Appl Phys* **89**, 988 (2001).
27. G.J. Conibeer, D.A. Woog, K.D. Rogers, D.W. Lane *14 European Photovoltaic Solar Energy Conference: Proceeding of the Conference*, 2075 (Munich: WIP-Renewable Energies: 1997).
28. M. Terheggen, H. Heinrich, G. Kostorz, A. Romeo, D. Baetzner, A.N. Tiwari, *E-MRS Spring Meeting* 345 (Strasbourg:E-MRS :2002).

## Вплив мікросекундного імпульсного гелієвого плазмового потоку на морфологію поверхні та кристалічну структуру фотоелектричних перетворювачів на основі CdS/CdTe

Г.С. Хрипунов<sup>1,2</sup>, М.М. Харченко<sup>1</sup>, А.В. Меріуц<sup>1</sup>, Ж.Ф. Карлен<sup>2</sup>, В.А. Махлай<sup>3</sup>, С.С. Геращенко<sup>3</sup>, С.Л. Абашин<sup>4</sup>, С.В. Суровіцький<sup>1</sup>, О.О. Пудов<sup>3</sup>, А.І. Доброжан<sup>1</sup>

<sup>1</sup> Національний технічний університет «Харківський політехнічний інститут», 61002 Харків, Україна

<sup>2</sup> Ecole Polytechnique Fédérale de Lausanne, CH-1015 Lausanne, Switzerland

<sup>3</sup> Національний науковий центр «Харківський фізико-технічний інститут», 61108, Харків, Україна

<sup>4</sup> Національний аерокосмічний університет «Харківський авіаційний інститут», 61070, Харків, Україна

Досліджено вплив імпульсного опромінення гелієвої плазми тривалістю 10 мкс і поверхневим енергетичним навантаженням  $0,2 \text{ МДж м}^{-2}$  на елементно-фазовий склад, морфологію поверхні та кристалічну структуру тонкоплівкових гетеросистем на основі CdS/CdTe. Шари сульфідів кадмію та телуриду кадмію були нанесені шляхом конденсації за допомогою методу гарячої стінки на скляну підкладку, покриту шаром FTO. Встановлено, що після одного імпульсу конструкція приладу залишається в робочому стані. Збільшення дози опромінення призводить до розпилення поверхні,

утворення наскрізних пор розміром 0,5 – 2 мкм і сітки мікротріщин з двома характерними лусочками. Одна сітка тріщин утворюється в скляній підкладці, а друга – з тріщинами в плівці CdTe. Показано, що теплова дія плазми стимулює дифузію сірки; внаслідок цього збільшується частка твердих розчинів CdTe<sub>1-x</sub>S<sub>x</sub>, що утворюються в процесі отримання гетеросистеми CdS/CdTe. Крім того, у цих твердих розчинах підвищується вміст сірки, що призводить до їх розкладання з виділенням фази твердого розчину CdS<sub>1-y</sub>Te<sub>y</sub>. Ці тверді розчини мігрують до поверхні CdTe через тріщини і спостерігаються як окремі кристали.

**Ключові слова:** Фотоелектричні перетворювачі, Тонка плівка, Телурид кадмію, Радіаційна стійкість, Тверді розчини.